Advanced on-line condition monitoring of, and inter-turn short circuit setectionin, power transformers

Aburaghiega, Ehnaish; Farrag, M E A; Hepburn, Donald; Garcia, Belen

Published in:
2018 53rd International Universities Power Engineering Conference (UPEC)

DOI:
10.1109/UPEC.2018.8542095

Publication date:
2018

Document Version
Author accepted manuscript

Advanced On-line Condition Monitoring of, and Inter-turn Short Circuit Detection in, Power Transformers

Ehnaish Aburaghiega* Ehnaish.Aburaghiega@gcu.ac.uk
Dr. Mohamed Emad Farrag*+ Mohamed.Farrag@gcu.ac.uk
Dr. D M Hepburn* dmhepburn_gcu@yahoo.com
Dr. Belen Garcia× bgarciad@ing.uc3m.es

*Glasgow Caledonian University, UK
+Faculty of Industrial Education, Helwan University, Egypt
×Universidad Carlos III de Madrid, Spain

***Abstract*—Transformers are an important part of any electrical power system network, warning of fault before failure is vital. The application of on-line fault detection reduces the cost of outages and the possibility of unpredicted failures. This paper outlines an electrically based on-line condition monitoring and short circuit detection method for power transformers. This method uses measurements of voltage and current in both sides of a transformer to classify its health and to identify fault conditions while in operation. Simulation results, relating to a number of short circuit winding faults, are analyzed and discussed. The results confirm that it is possible to identify a variety of short circuit conditions in primary and secondary windings from externally measurable parameters, i.e. measurement of voltages and currents in a transformer's windings can, based on available winding data, identify changes inside the transformer. The effect of load variation on the magnitude of the measured voltages and currents is also considered in this analysis.**

***Index Terms*—On-line condition monitoring, Short circuit, Voltages and currents, Fault detection, Loop current**

I. Introduction

Failure of a large transformer interrupts power supply to customers, resulting in high financial penalties, repair costs and environmental hazard. There has been a move from annual testing and off-line inspection to on-line condition monitoring of power transformers to eliminate these challenges and to extend transformer life cycle [1].

Power transformer reliability is dependent on the condition of its insulation system. The majority of transformers currently in service across the world were installed prior to 1980 and, as a result, many of them are approaching or have exceeded their designed life [2], [3]. As transformers are continuously subjected to electrical, thermal and mechanical stresses [4], degrading insulation is likely to result in an increased percentage of failures. Insulation failure, which is reputed to cause approximately 80% of transformer faults [5], can result in internal short circuit. Transformers, and associated network components, are at significant risk from failure due to this type of fault and methods for determining their existence are needed.

Understanding the transformer behavior and internal conditions when a short circuit exists has recently had significant attention from researchers, e.g. [6], [7]. Increasing concern regarding energy efficiency in the electricity supply grid, which may be affected as a result of transformer failure [8], has determined that advanced on-line diagnosis and fault detection should be applied.

Different techniques are used to investigate and understand the relationships between electrical signals and electrical and mechanical conditions [9], e.g. Sweep Frequency Response Analysis (SFRA) [10], Short-Circuit Impedance (SCI) [11], [12], Winding Resistance [13] or Finite Element method [14], [15]. In addition, poor mechanical strength of components and insulation may cause windings to collapse and deformation or damage to clamping structures [16] as a result of magneto-motive forces under short-circuit conditions. Wavelet Transform (WT) [17], Leakage Inductance Calculation [18] and short circuit test under Impulse Excitation [19] have been introduced to improve the accuracy of information collected for inter-turn short circuit fault detection. Many of these techniques require that units are taken out of the service for testing: operators would prefer that a transformer was not disconnected from the power grid.

To detect faults nearer inception, and to reduce the danger of transformer failure, on-line condition monitoring has become common. Different methods of determining the presence of inter-turn short circuit have been researched, e.g. extraction of winding parameters of a single-phase transformer based on primary and secondary currents and voltages [20], Transfer Function (TF) using time or frequency domain in [21]. This research applies continuous on-line condition monitoring to a transformer and indicates fault location and severity. These advantages are not available in the methods mentioned above.

In [22], the possibility of moving from off-line to on-line assessment of power transformers, based on internal short circuit detection, was outlined.

In this contribution, simulation of the behavior of a transformer under healthy and faulty conditions has been investigated. Parameters of a one to one transformer, 3 kVA, 230 V, 50/60 Hz, were measured and used to construct a model transformer. Simulation was used to investigate the application of the proposed on-line monitoring technique to detect faults of different severity based on measuring voltages and currents in both sides of the transformer during operation.

Initial measurements were taken of primary and secondary currents and voltages in the simulated healthy transformer. Subsequently, different section-to-section and inter-turn short circuits were introduced, and voltages and currents were determined accordingly. Thereafter, the data was assessed to compare the measured parameters of faulty and healthy transformers. The evolution of those variables with increasing fault severity is discussed and reported.

II. Transformer Construction

The main properties of the transformer, which was designed and manufactured to validate the proposed assessment method, are shown in Table I. A schematic of the transformer is shown in Fig. 1. Note that P.D1 to P.D4 and S.D1 to S.D4 refer to the Primary and Secondary winding Disc 1 to Disc 4, respectively. The transformer is a single-phase, shell type; the secondary sections are wound on the outside of the primary.

TABLE I
THE MAIN PROPERTIES OF THE TRANSFORMER

Primary/Secondary voltage	230/230 V
Power rating	3 kVA
Winding insulation type	Paper, 0.508 mm thickness
Insulation between windings	Screen, pressboard type
Cooling	Air, natural circulation

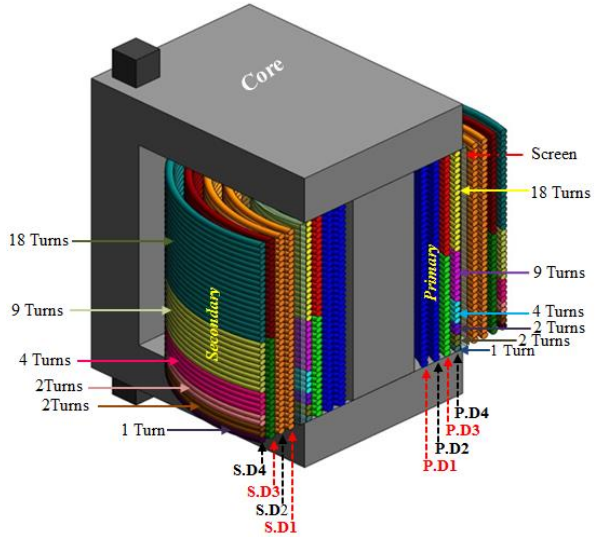

Fig. 1. Winding construction, showing discs and number of turns

Each disc of the Primary and Secondary windings has 36 turns. In both windings, as shown in Fig. 1, each layer of Disc 1 and 2 has 36 turns; Disc 3 has 2 sections of 18 turns, Disc 4 is divided into sections containing 18, 9, 4, 2, 2 and 1 turns.

III. Transformer Model and Simulation

The transformer model was simulated using PSPICE software, the simulation uses values of resistance (R), inductance (L) and capacitance (C) as measured in the winding sections of the practical transformer, parameters was collected from the transformer using appropriate devices. Simulation shows that the effects of capacitance are negligible at 50 Hz and that removing them from the model does not significantly affect results.

To investigate the operation of the healthy transformer under a range of load conditions, different resistive loads were applied to the model. Based on the transformer rated power of 3 kVA, and using Equation (1), different load percentages of the designed rated load have been calculated, different resistive loads of 15%, 30%, 45% and 60% of rated power were connected in the simulation.

$$S\% = \frac{S}{S_{rated}} \times 100 \quad (1)$$

Where S and S_{rated} are, respectively, the load power and the transformer rated power.

Voltages and currents were recorded in both sides of the healthy transformer for the four load conditions, as shown in Table II. In all cases 230 V was applied to the transformer primary. As it is expectable, as the load increases the primary and secondary currents increase and the secondary winding voltage reduces because of the transformer internal voltage drop, this behavior is expected for a practical transformer too

TABLE II
SIMULATION DATA FOR ELECTRICAL VARIABLES UNDER DIFFERENT LOADS

Load	Resistive load (Ω)	I_{in} (A)	V_{out} (V)	I_{out} (A)
15 %	114.00	2.29	226.40	1.98
30 %	56.00	4.31	222.78	3.98
45 %	36.36	6.26	219.08	6.02
60 %	26.25	8.41	215.15	8.19

IV. Study of Primary Winding Faults

The simulation and test procedure, validated by the healthy transformer, was applied to a model in which short circuit faults had been created. Different numbers of shorted turns were introduced into both primary and secondary windings. Additional investigation and simulation tests were conducted in order to understand the internal and external changes of the transformer currents and voltages under different fault conditions.

A. Short Circuit Calculation

Calculations determined the voltages that could be safely applied in the transformer with shorted turns, given that primary, secondary and short circuit currents should not exceed the transformer rated current of 13 A. The voltage applied in the simulation was set to 10.7 V, the load was simulated as three 150 Ω resistances connected in parallel.

IEC standards [23], [24] define the formulae for calculating *arc* resistance, as stated in Equation (2), and used, e.g. in [35].

$$R_l = 1.05 \times \frac{L}{I}\ (\Omega) \quad (2)$$

Where: L – *arc* length in meters, I – current in Amps.

In practical validation tests, wire links are used to provide a short circuit current path, so the current can by-pass shorted turns as would occur in an *arc*. As mentioned earlier, the values for simulating the transformer were collected from a real transformer: based on Equation (2), tests were conducted to determine the wire link resistance value which should be used to simulate an *arc* for the practical transformer. It is found that using a resistance of 1.25 m Ω would ensure that the applied resistance is always less than the calculated *arc* resistance, the wires functioning as the *arc* path should give good indication of the system performance under practical

tests. Simulations used the wire resistance values to ensure compatibility of data.

B. *Primary winding faults*

As discussed in Section III, the transformer model was simulated using PSPICE. Fig. 2 shows a truncated version of the transformer model.

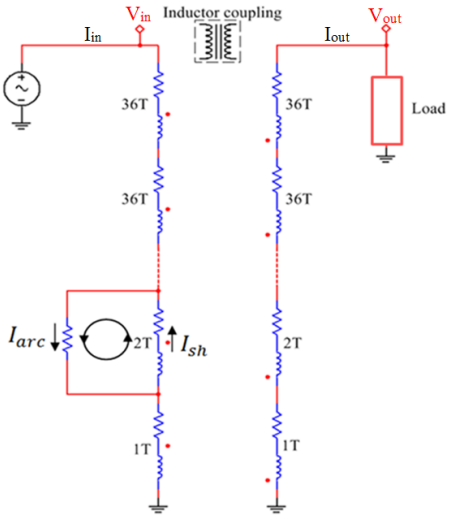

Fig. 2 PSPICE simulated transformer with two turns short circuited

The values for the simulated primary and secondary winding voltages and currents under each fault were recorded.

Results from simulation of the healthy transformer and for different numbers of shorted turns in the primary winding can be seen in Table III. A higher number of shorted turns in the primary winding led to an increase in the primary winding current: the level of increase depends on the number of the shorted turns. The reason for the increased primary winding current during the fault is the localized reduction in winding impedance, caused by the very low Ohmic value in the *arc* across the shorted turns. It is worth noting that faults with the same number of shorted turns have the same effect on the measured values, i.e. it is not possible to identify the location of a fault from the changes of voltage and current.

TABLE III
DATA OF THE PRIMARY WINDING SHORT CIRCUIT VARIABLES

Number of Shorted turns	I_{in} (A)	V_{out} (V)	I_{out} (A)
Healthy	0.21	10.32	0.21
1	0.22	10.32	0.21
2	0.24	10.32	0.21
2	0.24	10.32	0.21
4	0.32	10.32	0.21
9	0.72	10.32	0.21
18	2.08	10.32	0.21
18	2.08	10.32	0.21
18	2.08	10.32	0.21
36	5.62	10.32	0.21
36	5.62	10.32	0.21

From Table III, it is clear that primary current can be used as the main indicator for a primary winding short circuit. It is also found that neither the secondary voltage nor secondary current are affected when the fault occurs in the primary winding.

C. *Analysis of Faulty Primary Winding*

To investigate the internal variations responsible for changes at the transformer's input and output for primary winding faults, the internal currents in a faulty transformer were studied. Fig. 2 shows a part schematic of the simulated transformer with two turns short circuited, I_{arc} represents the current in the *arc* and I_{sh} represents the current in the shorted turns. Analyzing the currents due to shorted turns in the primary winding allows interpretation of the relationship between internal and external currents in a faulty transformer.

The following test steps were applied:

1) Simulate a healthy transformer and measure primary winding current I_{in},
2) For each number of turns short circuited, record the primary current I_{in}, the shorted turns current I_{sh} and for the *arc* I_{arc}.
3) Analyze the test results.

As an example, the data collected from a healthy transformer and faulty with two turns short circuited are compared and analyzed below. The difference between the healthy and faulty primary winding current measured was calculated using Equation (3).

$$\Delta_i = I_{in}.F - I_{in}.H \quad (3)$$

Where Δ_i is the difference between the primary winding current in a fault case, $I_{in}.F$, and a healthy case, $I_{in}.H$.

The simulated primary winding current $I_{in}.F$ and that in the *arc* I_{arc} and in the shorted turns I_{sh} are presented in Fig. 3. It can be seen that both fault currents are higher than the input current. It is also noted that while the primary winding and *arc* currents flow in the same direction, the current in the shorted turns flows in the opposite direction.

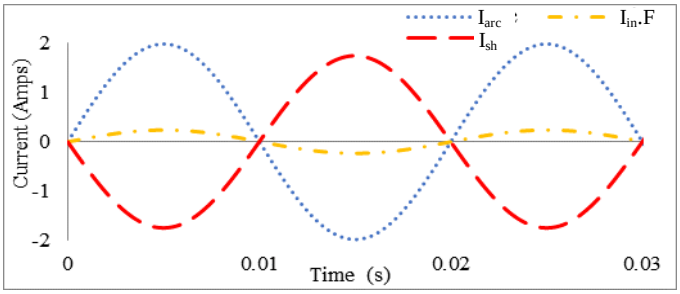

Fig. 3 Comparison of the primary winding current and the currents at the fault location in the primary winding

From Kirchoff's Laws the primary winding current is the vector sum of the currents flowing in the *arc* and shorted turns, as stated in Equation (4).

$$I_{in}.F = I_{arc} + I_{sh} \quad (4)$$

As Fig. 3 shows, the data collected are in agreement with Equation 4.

Table III shows that as the number of shorted turns increases the magnitude of the primary current increases, incrementing the number of shorted turns also lead to increase the loop current I_{arc} and I_{sh}. Note that, even though faulty primary currents stay below a transformer's rated current, the loop current can be damagingly high. High temperatures generated by Ohmic losses may damage the transformer insulation.

D. Interpretation of the High Loop Current

Theoretically, windings are connected through a complex mutual network related to the winding inductances. Due to failed insulation, an *arc* current can travel between two points in the winding: this *arc* crosses the mutually inductive network that links the windings, as illustrated in Fig. 4. The P-to-S Links represent the inductive links between the Primary and Secondary windings and the P-to-P Links are those between turns in the primary coil.

The alternative current path provided by the *arc* permits the formation of a closed circuit at the fault location and a loop current is induced.

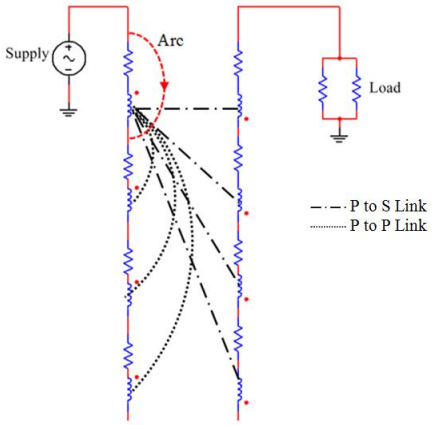

Fig. 4 Inductor coupling network and *arc* current for one shorted turn

To confirm that the loop current at the fault location was generated as a result of magnetic coupling in the transformer windings, PSPICE simulations were conducted in which the inductive coupling related to the shorted turns was cancelled, i.e. the shorted turns are not mutually connected to the remaining turns in the primary and secondary windings.

The outcome of the simulation indicates that, in the practical transformer, the magnetic circuit is responsible for generating the loop current at the fault location.

E. Study and Simulated Results

Using simulation, The relationship between the internal and external voltages and currents in a transformer has been studied. Short circuits of 1 to 36 primary turns were investigated. Data for the currents $I_{in}.F$, I_{sh} and I_{arc}, are shown in Table IV: note that $I_{arc} > I_{sh}$. As the impedance of the faulty coil reduces with higher numbers of shorted turns, the primary winding current will therefore increase.

Although the low supply voltage keeps the primary winding current below the transformer rated current of 13 A for the majority of cases, for 36 shorted turns the local current in the shorted turns exceeds the rated current.

The relationships between fault magnitude (number of shorted turns) and measured currents $I_{in}.F$ and I_{sh}, are shown in Fig. 5. Equations (5) and (6) represent these relationships.

TABLE IV
PRIMARY WINDING CURRENT AND CIRCULATING CURRENTS FOR PRIMARY WINDING FAULTS

Number of shorted turns	I_{in}-F (A)	I_{sh} (A)	I_{arc} (A)
1	0.22	0.99	1.21
2	0.24	1.75	1.99
4	0.32	3.63	3.95
9	0.72	7.44	8.16
18	2.08	12.93	15.00
36	5.62	16.24	21.86

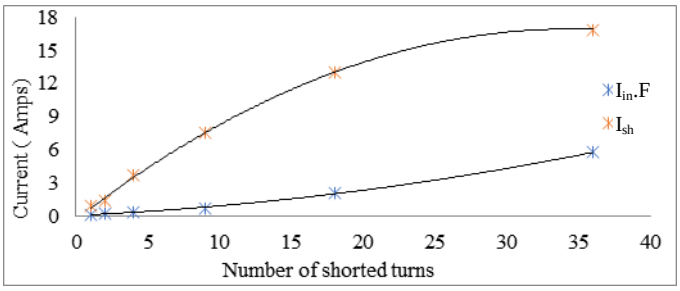

Fig. 5 Relationships between I_{in}-F and I_{sh} and number of shorted turns, obtained from simulation data.

$$I_{in}.F = 0.0028x^2 + 0.0578x + 0.1209 \quad (5)$$

$$I_{sh} = -0.0144\,x^2 + 0.9934x + 0.117 \quad (6)$$

Where $\boldsymbol{x}$ is the number of the shorted turns.

Equation (5) can be used, for this transformer, to determine the number of shorted turns, $\boldsymbol{x}$, from the value of $I_{in}.F$. The value of $\boldsymbol{x}$ can then be used to calculate with Equation (6) the magnitude of internal current, I_{sh}, and, with Equation (4), I_{arc}.

As the load connected to the simulated transformer can vary, resistive load variation effects on a faulty transformer were simulated. As expected, increasing load results in higher values of current in the primary winding and the circulating loop. Fig. 6 shows loop current variation due load change for one shorted turn in the primary winding. Note that the load percentage was calculated using Equation (1). This confirms that fault effects become greater as load increases, due to increasing magnitudes of local currents. Increasing current magnitudes would have a detrimental effect on the insulation.

As outlined earlier, this contribution aims to classify a transformer's condition based on measured primary and secondary voltages and currents. The load variation simulation on a healthy transformer shows that the input and output currents increase as the load increases; see Table II. However, as discussed in IV-*B*, while a short circuit in the

primary coil causes primary current to increase the secondary current is not affected. Therefore, the difference between primary and secondary currents can indicate whether the transformer is healthy or a short circuit exists.

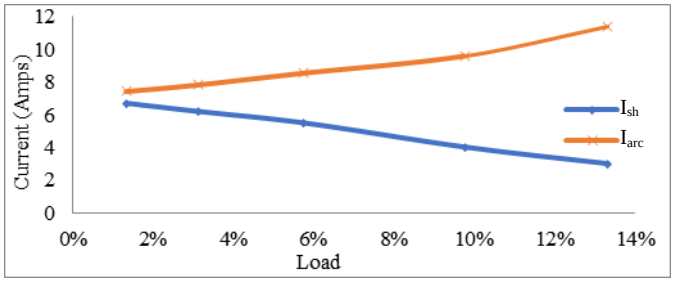

Fig. 6 Loop currents for increasing load for 1 shorted turn in primary winding

V. Study of Secondary Winding Faults

A. Simulated results

The procedure applied for primary winding fault indication in Section IV was applied to the secondary winding. As previously, 10.7 V is applied to the simulated transformer. Voltage and current data were collected from both transformer windings for different number of shorted turns in the secondary side, see Table V.

TABLE V
VALIDATION OF THE SECONDARY WINDING SHORT CIRCUIT VARIABLES

Number of shorted turns	I_{in} (A)	V_{out} (V)	I_{out} (A)
Healthy	0.21	10.320	0.217
1	0.22	10.260	0.205
2	0.23	10.170	0.203
2	0.23	10.170	0.203
4	0.31	9.970	0.199
9	0.67	9.304	0.186
18	1.63	7.911	0.158
18	1.63	7.911	0.158
18	1.63	7.911	0.158
36	3.74	5.320	0.111
36	3.74	5.320	0.111

The tests confirm that shorting similar numbers of turns in different locations in the coil has similar effects on the measured factors. As with primary winding faults, it is possible to determine that a defined magnitude of fault exists but not the fault location.

Fig. 7 and Fig 8 present the changes in primary winding current I_{in}, secondary winding voltage V_{out} and the secondary winding current I_{out}, respectively, for different numbers of shorted turns. There is a significant variation in the current and voltage values as the number of shorted turns increases.

The relationship between measured data and number of shorted turns can be identified using Equations (7), (8) and (9), where x is the number of shorted turns. Based on measured data, the number of shorted turns can be identified and the fault severity known.

As the number of shorted turns in the secondary winding increases the primary current increases, however the secondary voltages and currents decrease. This indicates that for the practical transformer, and other transformers that were similarly simulated, it would be possible to identify the magnitude of a fault in the secondary side of a transformer using the three measurements.

$$I_{in} = 0.0015x^2 + 0.0485x + 0.165 \quad (7)$$

$$V_{out} = -0.0008x^2 - 0.1115x + 10.147 \quad (8)$$

$$I_{out} = -1e\text{-}05x^2 - 0.0022x + 0.2006 \quad (9)$$

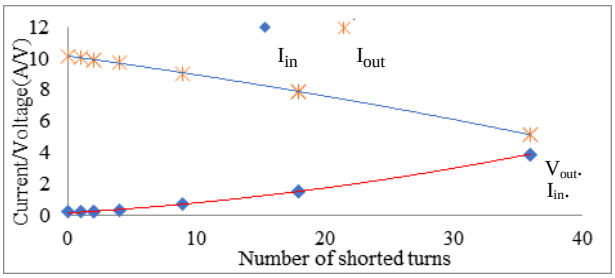

Fig. 7 The relationship between (i) the primary winding current and (ii) secondary voltage and number of shorted turns in the secondary coil

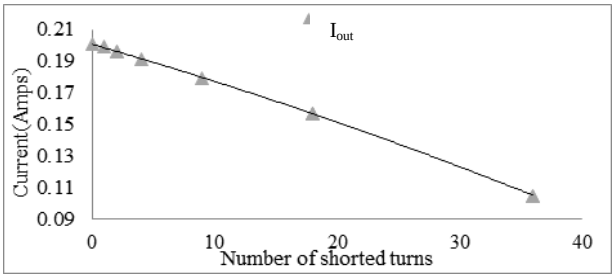

Fig. 8 The relationship between the secondary winding current and the number of shorted turns in the secondary coil

B. Investigation of the faulty secondary winding conditions

The simulations in Section IV-*C* are repeated for short circuits in the secondary winding. As previously, analysis of a healthy transformer determined initial I_{in}, I_{out}, V_{out}, for a faulty transformer I_{arc} and I_{sh} are also measured. Note that all data are rms values.

As indicated above, a short circuit in a secondary coil causes the primary current to increase and the secondary voltage and current to decrease. As before, impedance changes cause changes in I_{in} and the internal current is due to magnetic coupling effects. In contrast to the primary coil faults, as $I_{sh} > I_{arc}$, I_{sh} is in the same direction as the secondary current and I_{arc} flows in the opposite direction to I_{sh}.

From Fig. 7 and 8, the secondary voltage and current are reduced due to the decrease in inductive coupling. As discussed in Section IV-*D*, the inductive coupling related to the shorted turns were cancelled in simulation and results show that the current in the shorted turns became zero, and the secondary current becomes I_{arc}.

C. Analysis of Faulty Secondary Winding

For the secondary winding short circuit tests, the measured variables for different numbers of shorted turns are given in Table VI. Simulation confirms that I_{sh} is higher than I_{arc} for this type of fault, which would result in higher temperatures

in the coil and potential damage to the insulation.

Analysing the data in Table VI allows the relationship between the number of shorted turns and I_{arc} and I_{sh} to be developed. The number of shorted turns x can be found from the measured output current using Equation (9). I_{sh} and I_{arc} can be found using Equations (10) and (11), respectively.

$$I_{sh} = -0.0112x^2 + 0.8043x + 0.4314 \quad (10)$$

$$I_{arc} = -0.0112x^2 + 0.8066x + 0.2308 \quad (11)$$

TABLE VI
WINDING AND LOOP CURRENTS FOR SECONDARY WINDING FAULTS

Number of shorted turns	I_{out} (A)	I_{sh} (A)	I_{arc} (A)
1	0.205	1.104	0.899
2	0.203	2.167	1.964
4	0.199	4.060	3.861
9	0.186	7.850	7.664
18	0.158	11.921	11.763
36	0.111	14.613	14.502

VI. CONCLUSION

This work confirms that definable changes in voltages and currents of a transformer occur when short circuits exist in either primary or secondary winding. Primary winding faults can be detected by comparison with healthy values, e.g. a 2 turn fault would change current by 14.6%. A similar fault in the secondary winding affects both primary and secondary currents and the secondary voltage, this leads to changes of 10.10%, -10.10% and -2.32%, respectively.

Although the number of shorted turns and the magnitudes of local currents can be found from measured values, information about fault location cannot be provided.

While external currents in a faulty transformer may be below rated values, local loop currents may not. This could lead to further insulation degradation and mechanical problems.

Voltages and currents in both sides of a transformer can be defined for different loads if the winding details are known.

The method presented here should, using appropriate measured variables, be applicable to other transformers. Monitoring and evaluation of electrical variables can be carried out after performing an initial study to determine the influence of construction on the measured variables.

Continuous measurement and analysis of electrical variables can usefully complement other assessment methods to provide real time indication of a transformer's condition.

REFERENCES

[1] "IEEE Guide for the Application and Interpretation of Frequency Response Analysis for Oil-Immersed Transformers IEEE Power and Energy Society," *IEEE Std C57.149™-2012*, no. March, 2013.

[2] N. Hashemnia, A. Abu-Siada, and S. Islam, "Detection of Power Transformer Bushing Faults and Oil Degradation using Frequency Response Analysis," *IEEE Trans. Dielectr. Electr. Insul.*, vol. 23, no. 1, pp. 222–229, 2016.

[3] N. Abeywickrama, Y. Serdyuk, and S. Gubanski, "Effect of core magnetization on frequency response analysis (FRA) of power transformers," *IEEE Trans. Power Deliv.*, vol. 23, no. 3, pp. 1432–1438, 2008.

[4] S. Akolkar and B. Kushare, "Remaining Life Assessment of Power Transformer," *J. Autom.& Contr*, vol. 2, no. 2, pp. 45–48, 2014.

[5] O. Aljohani and A. Abu-Siada, "Application of Digital Image Processing to Detect Short-Circuit Turns in Power Transformers using Frequency Response Analysis," *IEEE Trans. Ind. Informatics*, vol. 12, no. 6, pp. 2062–2073, 2016.

[6] L. Oliveira and A. Marques Cardoso, "Leakage Inductances Calculation for Power Transformers Interturn Fault Studies," *IEEE Trans. Power Deliv.*, vol. 30, no. 3, pp. 1213–1220, 2015.

[7] D. Zacharias and R. Gokaraju, "Prototype of a Negative Sequence Turn-to-Turn Fault Detection Scheme for Transformers," vol. 31, no. 1, pp. 122-129, 2016.

[8] M. Erol-Kantarci and H. Mouftah, "Energy-Efficient Information and Communication Infrastructures in the Smart Grid: A Survey on Interactions and Open Issues," IEEE Commun. Surv & Tutorials, vol. 17, no. 1, pp. 179–197, 2015.

[9] J. Kumar and U. Perasadr, "Expert System for Sweep Frequency Response Analysis of Transformer Using MATLAB," *Inter. Jou. Scien. & Resea. public*, vol. 2, no. 12, pp. 1–13, 2012.

[10] J. Gonzales and E. Mombello, "Fault Interpretation Algorithm Using Frequency-Response Analysis of Power Transformers," *IEEE Trans. Power Deli*, vol. 31, no. 3, pp. 1034–1042, 2016.

[11] Y. Liu *et al.*, "A study of the sweep frequency impedance method and its application in the detection of internal winding short circuit faults in power transformers," *IEEE Trans. Dielectr. Electr. Insul.*, vol. 22, no. 4, pp. 2046–2056, 2015.

[12] A. Palani *et al*, "Real-time techniques to measure winding displacement in transformers during short-circuit tests," *IEEE Trans. Power Deliv.*, vol. 23, no. 2, pp. 726–732, 2008.

[13] H. Mirzaei *et al* , "Advancing new techniques for UHF PDdetection and localization in the power transformers in the factory tests," *IEEE Trans. Dielectr. Electr. Insul.*, vol. 22, no. 1, pp. 448–455, 2015.

[14] J. Liu and V. Dinavahi, "Nonlinear Magnetic Equivalent Circuit-Based Real-Time Sen Transformer Electromagnetic TransientModel on FPGA for HIL Emulation," *IEEE Trans. Power Deliv.*, vol. 31, no. 6, pp. 2483–2493, 2016.

[15] D. Geissler and T. Leibfried, "Short Circuit Strength of Power Transformer Windings - Verification of Tests by a Finite Element Analysis Based Model," *IEEE Trans. Power Deliv.*, vol. X, no.Y, pp. 1–8, 2016.

[16] G. Kumbhar and S. Kulkarni, "Analysis of short-circuit performance of split-winding transformer using coupled field-circuit approach," *IEEE Trans. Power Deliv.*, vol. 22, no. 2, pp. 936–943, 2007.

[17] R. Medeiros, F. Costa, and K. Silva, "Power Transformer Differential Protection Using the Boundary Discrete Wavelet Transform," *IEEE Trans. Power Deliv*, vol. 31, no. 5, pp. 2083–2095, 2016.

[18] M. Lambert *et al*, "Analytical calculation of leakage inductance for low-frequency transformer modeling," *IEEE Trans. Power Deliv.*, vol. 28, no. 1, pp. 507–515, 2013.

[19] P. Rajamani and S. Chakravorti, "Identification of simultaneously occurring dynamic disc-to-disc insulation failures in transformer winding under impulse excitation," *IEEE Trans. Dielectr. Electr. Insul.*, vol. 19, no. 2, pp. 443–453, 2012.

[20] P. Reddy and B. Rajpurohit, "On-Line Monitoring of Winding Parameters for Single-Phase Transformers," *IEEE 6th India Inter. Conf. on Power Electro*, pp. 1–4, 2014.

[21] T. De Rybel, *et al*, "Apparatus for online power transformer winding monitoring using bushing tap injection," *IEEE Trans. Power Deliv.*, vol. 24, no. 3, pp. 996–1003, 2009.

[22] E. Aburaghiega, M. Farrag, D. Hepburn and B. Garcia, "Power Transformer Health Monitoring : A shift from off-line to on-line detection," *50th Inter.(UPEC)*, pp. 1-6, 2015.

[23] CIGRE Study Committee 13-01. WG01, "Application of black box modelling to circuit breakers," 1993.

[24] S. Bjelic, N. Markovic and U. Jaksic, "The simplified procedure for calculation of Influence of thermal losses on decrease of technical endurance of electric equipment," *in 3. Regional Conf. Indus. Energy & Envir. Protection in Southeastern Europe IEEP'11*, 2011, pp. 21–25.

[25] N. Markovic, S. Bjelic, J. Zivanic and U. Jaksic, "Numerical simulation and analytical model of electrical arc impedance in the transient processes," *Prz. Eelcktrotechniczny*, no. 2, pp. 113–117, 2013.